



## Dynamic adsorption of In(III) and Fe(III) on solvent impregnated resins containing trioctylmethylammonium chloride

Xuezen Gao, Junshen Liu\*, Xunyong Liu, Lei Guo, Shengxiao Zhang

School of Chemistry and Materials Science, Ludong University, Yantai 264025, China, Fax: +86 535 6697537; emails: liujunshen@163.com (J.S. Liu), gaoxuez@163.com (X.Z. Gao), xunyongliu@126.com (X.Y. Liu), unikguo@gmail.com (L. Guo), beijingzxs@163.com (S.X. Zhang)

Received 31 August 2020; Accepted 29 January 2021

### ABSTRACT

Solvent impregnated resins (SIRs) were prepared by dry impregnation using styrene-divinylbenzene type macroreticular resin (HZ-818) as support and trioctylmethylammonium chloride as extractant. Adsorption and separation performance of In(III) and Fe(III) with SIRs was studied on HCl medium by static and dynamic adsorption method. The effect of HCl concentration on the adsorption of In(III) and Fe(III) was investigated by static adsorption method. The effect of feed flow rate, bed height, and metal ion concentration (In(III) and Fe(III)) was investigated by dynamic adsorption method. The optimized acidity for In(III) and Fe(III) adsorption with SIRs was 4 mol/L HCl in single-component and bi-component systems containing In(III) and Fe(III). The dynamic adsorption study revealed that when the concentration of HCl, feed flow rate, bed height, and metal ion concentration were 4 mol/L, 1.4 mL/min, 140 mm, and 90 mg/L at ambient temperature, the adsorption capacities of In(III) and Fe(III) in single-component system were 13.1 and 37.8 mg/g, respectively, and the adsorption capacities of In(III) and Fe(III) in bi-component system were 1.3 and 35.8 mg/g, respectively. Hence, SIRs could selectively adsorb Fe(III), and the separation of In(III) and Fe(III) in HCl solution could be achieved.

*Keywords:* Solvent impregnated resins; Adsorption; Separation; In(III); Fe(III); Dynamic adsorption method

### 1. Introduction

Indium, as a crucial element for a wide variety of high-technology applications, is increasingly used in electronic devices [1–3]. The content of indium in the Earth's crust is low and dispersed. This element is associated with sulfide deposits and tin-polymetallic-zinc deposits [4,5]. In addition, indium can be recycled from waste electronic products, such as liquid crystal displays [6,7]. A large number of impurity ions exist in the process of purifying indium from these resources by hydrometallurgy. Typical impurity ions are usually Zn(II), Fe(III), Cu(II), Sn(II) and so on. Among these metal ions, Fe(III) is often reduced to Fe(II) to

eliminate interference before recovering indium [8,9], and the process requires a large amount of reducing agent.

Technologies for separating and recovering In(III) include precipitation, electrochemical recovery, solvent extraction and adsorption on resin [10–13]. Solvent extraction is the most widely used method for purification of In(III) in process metallurgy. However, there are the problems of loss of extractant and consumption of large amounts of organic solvent.

Among these methods, adsorption on resin has been used widely because it is simple, economical, and cost-effective. Solvent impregnated resins (SIRs) combine the advantages of solvent extraction and ion exchange resins

\* Corresponding author.

[14]. SIRs are prepared with extractant and macroporous resins. The extractant is loaded into macroporous resin by physical adsorption [15]. Compared with solvent extraction, SIRs have the advantages of reducing the dispersion of the extractant, the pollution of organic solvents, and the formation of emulsions [16,17]. In addition, SIRs can adsorb and separate metal ions by dynamic adsorption (column adsorption). SIRs can be designed and prepared by selecting different extractants and macroporous resins [18]. The extractant, which can be selected through the solvent extraction experiment, is one of the most important factors for separating and recovering metal ions.

Extractants for In(III) and Fe(III) recovery by solvent extraction can be classified into three types: acidic, neutral, and basic extractants. The acidic extractants and neutral extractants are the most widely used for In(III) and Fe(III) recovery, particularly organophosphate extractants. Examples of extractants for In(III) recovery are di-(2-ethylhexyl) phosphoric acid (D2EHPA), 2-ethylhexyl phosphonic acid mono 2-ethylhexyl ester (EHEHPA), bis(2,4,4-trimethylpentyl) phosphinic acid (Cyanex 272), tri-*n*-butyl phosphate (TBP), and organophosphine oxide (Cyanex 923) [12,19–21]. D2EHPA, EHEHPA, and Cyanex 923 have been used to prepare SIRs for In(III) or Fe(III) adsorption [22–24]. These extractants have high loading capacities for In(III) or Fe(III) but have poor selectivity for In(III) and Fe(III). In addition, most acidic extractants used to recover Fe(III) are difficult to strip Fe(III) from the supported organic phase [25–27].

Basic extractants refer primarily to amine extractants. Compared with acidic and neutral extractants, fewer studies have investigated on using amine extractants extraction of In(III) and Fe(III). However, amine extractants have higher extraction rate and better selectivity for extracting Fe(III) [28]. The third phase will appear during solvent extraction process with amine as the extractant. Separating aqueous and organic phases is difficult, thereby restricting the application of amine extractants [28]. As an amine extractant, trioctylmethylammonium chloride containing quaternary ammonium functional groups ( $\text{CH}_3\text{R}_3\text{N}^+$ ) was used as a phase transfer catalyst and metal extractant. This extractant showed good extraction capacity for metals. Mishra et al. [29] used trioctylmethylammonium chloride as the extractant to extract Fe(III) from HCl leach liquor by solvent extraction. The extracted species of Fe(III) was  $\text{R}_3\text{NCH}_3\cdot\text{FeCl}_4$ . The extraction rate of Fe(III) was 98.57% in two-counter-current stages with 0.2 mol/L trioctylmethylammonium chloride at 1:1 phase ratio. Cui et al. [30] reported that sodium sulfite as eluent can effectively strip off Fe(III) from trioctylmethylammonium chloride loaded with Fe(III). When the temperature was 50°C and the phase ratio (O/A) was 1:2, the elution rate of 0.8 mol/L sodium sulfite was approximately 95%. Inoue and Alam [31] prepared SIRs with trioctylmethylammonium chloride as extractant. The prepared SIRs were used to recover In(III) from flat-panel displays. Study found that trioctylmethylammonium chloride SIRs could selectively adsorb Fe(III) without adsorbing In(III) in 3 mol/L HCl leach liquor. Roosendaal et al. [32] prepared a supported ionic liquid phase with the iodide form of trioctylmethylammonium chloride, which can selectively adsorb In(III) in the Fe(III) and In(III) mixed solution. These reported the adsorption performance of

trioctylmethylammonium chloride to adsorb Fe(III) or In(III) but did not systematically investigate the adsorption performance of In(III) and Fe(III) by dynamic adsorption method in single-component and bi-component systems.

In this study, trioctylmethylammonium chloride was chosen as extractant, and SIRs were prepared with trioctylmethylammonium chloride and styrene-divinylbenzene type macroporous resin (HZ-818) by dry impregnation. The effect of HCl concentration on the adsorption performance of In(III) and Fe(III) was studied by static adsorption method. The adsorption and separation performance of SIRs for In(III) and Fe(III) in HCl medium was systematically studied by dynamic adsorption method. The effects of feed flow rate, bed height, and metal ion concentration were investigated by dynamic adsorption method. As a result of this research, an efficient method was proposed to separate In(III) and Fe(III) by SIRs technique.

## 2. Materials and methods

### 2.1. Instrumentation

Scanning electron microscope (SEM) images of SIRs were recorded on JSF5600LV (JEOL, Japan). Thermogravimetry analysis (TGA) was conducted on TG 209 Thermal Analyzer (Netzsch, Germany). Fourier transform infrared spectra (FTIR) were recorded on Nicolet MAGNA IR 550 (series II). In the single-component system, the concentration of metal ions was determined with UV-2550 spectrophotometer (Shimadzu, Japan). In the bi-component system, the concentration of metal ions was determined with 932A-model atomic adsorption spectrometer (GBC, Australia) equipped with nitrous oxide-acetylene flame.

### 2.2. Materials and reagents

Trioctylmethylammonium chloride extractant with 95% purity was purchased from Shanghai Rare-earth Chemical Co., Ltd, China. The molecular structure of trioctylmethylammonium chloride is shown in Fig. 1. HZ-818 macroporous resin, a styrene-divinylbenzene type support, was purchased from Shanghai Huazhen Polymer Co., Ltd, China. The bead size of HZ-818 is 20–60 mesh. Other reagents used were of analytical grade and used directly.

### 2.3. Preparation of SIRs

Before impregnation, HZ-818 resin was first treated with absolute ethanol and 5% HCl solution to remove inorganic impurities and monomer materials. Then, the resins were thoroughly rinsed with deionized water and dried in a drying oven at 323 K for 12 h. SIRs were prepared by dry impregnation method. In brief, 15.02 g of pre-treated HZ-818 resins were immersed in 60 mL of trioctylmethylammonium chloride and ethanol mixed solution (the volume ratio: 1:1). The mixture was stirred for 48 h to complete the impregnation process at 313 K. The SIRs were then separated by vacuum suction filtration, rinsed with deionized water, and evaporated at 323 K in the drying oven. A total of 25.01 g of SIRs were obtained. The amount of trioctylmethylammonium chloride of SIRs was determined

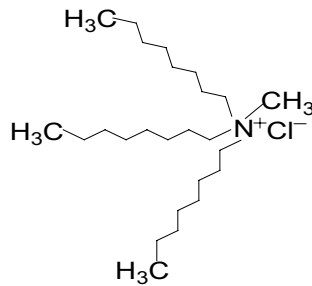


Fig. 1. Molecular structure of trioctylmethylammonium chloride.

based on change in the weight of the resins before and after impregnation. The content of trioctylmethylammonium chloride per gram of SIRs is 0.40 g.

#### 2.4. Sorption studies

##### 2.4.1. Effect of HCl concentration

The effect of HCl concentration was studied by static adsorption method in the single-component system (In(III) or Fe(III)) and bi-component system (In(III) and Fe(III)). In static adsorption, 0.0250 g of SIRs were shaken with 25.0 mL of metal ion solution to the equilibrium in constant temperature bath oscillator. The concentration of metal ions before and after adsorption was analyzed. The adsorption capacity of metal ions on SIRs ( $Q$ , mg/g) was calculated by Eq. (1). The distribution ratio ( $D$ , L/g) was calculated by Eq. (2). The separation coefficient  $\beta$  of In(III) and Fe(III) was calculated by Eq. (3).

$$Q = \frac{(C_0 - C_e)V}{m} \quad (1)$$

$$D = \frac{C_0 - C_e}{m} \frac{V}{C_e} = \frac{Q}{C_e} \quad (2)$$

$$\beta = \frac{D_{\text{Fe}}}{D_{\text{In}}} \quad (3)$$

where  $C_0$  is the initial concentration (mg/L),  $C_e$  is the equilibrium concentration (mg/L),  $V$  is the volume of solution (L), and  $m$  is the mass of SIRs (g).

##### 2.4.2. Dynamic adsorption

The adsorption experiment of SIRs by dynamic adsorption method was carried out in a glass column (250 mm × 3.0 mm i.d.). A known amount of SIRs was swollen previously and then packed in column by wet method. The adsorption column was activated with 4 mol/L HCl solution before metal ions adsorption. The metal ion solution was pumped into the column at a certain flow rate through a peristaltic pump. Effluent was collected at regular intervals. The concentration of the effluent samples was recorded continuously. The experimental scheme of the dynamic adsorption of SIRs in single-component and bi-component system is shown in Fig. 2. Dynamic adsorption capacity ( $Q$ , mg/g) was calculated with Eq. (4).

$$Q = \frac{\sum(C_0 - C_i)V_i}{m} \quad (4)$$

where  $C_0$  and  $C_i$  are the initial and effluent sample concentrations (mg/L) of metal ions, respectively;  $V_i$  is the volume of the effluent sample (L), and  $m$  is the mass of the SIRs (g).

##### 2.4.3. Dynamic elution

SIRs loaded with metal ions were first washed with 4 mol/L HCl solution until the washing effluent is free of metal ions and then regenerated by HCl solution with pH 1.0, 2.0, and 2.5. The concentration of the effluent samples was recorded during the regeneration step. Dynamic elution rate ( $E$ , %) was calculated using Eq. (5).

$$E = \frac{\sum C_i V_i}{mQ} \times 100 \quad (5)$$

where  $C_i$  is the effluent sample concentration (mg/L) of the metal ions,  $Q$  is the adsorption capacity (mg/g),  $V_i$  is the volume of the effluent sample (L), and  $m$  is the mass of the SIRs (g).

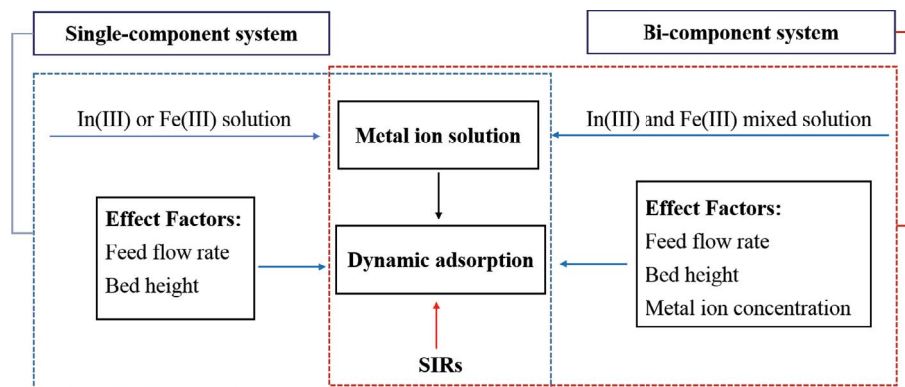


Fig. 2. Experimental scheme of the dynamic adsorption of SIRs in single-component and bi-component systems.

### 3. Results and discussion

#### 3.1. Characterization of SIRs

##### 3.1.1. Scanning electronic microscopy analysis

The surface morphology and cross-section morphology of HZ-818 and SIRs were characterized by SEM. As shown in Fig. 3a and b are the surface morphology of HZ-818 resins and SIRs, respectively; and a' and b' are the cross-section morphology of HZ-818 resins and SIRs, respectively. Comparison of the surface morphology of HZ-818 resins and SIRs showed that they have regular spherical structure. Comparison of the cross-section morphology of HZ-818 resins and SIRs indicated that the smoother morphology of SIRs.

##### 3.1.2. Thermogravimetry analysis

The thermal properties of SIRs were analyzed by thermogravimetry from 25°C to 800°C. Thermal stability and applicable temperature were evaluated. Fig. 4 shows the thermogravimetry analysis curves of SIRs. The temperature where SIR has substantial weight loss is lower than that of HZ-818. The loss between ambient temperature and 121°C for SIRs is due to the dehydration of physically adsorbed water. The loss between 172°C and 340°C for SIRs is due to the decomposition of trioctylmethylammonium chloride. The third weight loss of SIRs was observed within 320°C–480°C due to the decomposition of HZ-818. Although the main weight loss stage of SIR was significantly decreased at 172°C, the utilization of the adsorbent was slightly affected due to the low temperature for common adsorption operations.

##### 3.1.3. Fourier transform infrared spectroscopy analysis

The infrared spectra of SIRs are shown in Fig. 5. Based on the infrared spectra of HZ-818 resin, the stretching

vibrational band of C–H ( $-\text{CH}_2$ ) bond and C–N bond appeared at 2,855.8 and 1,376.6  $\text{cm}^{-1}$  in Fig. 5b, respectively. This finding indicated that trioctylmethylammonium chloride was successfully impregnated on HZ-818 resin.

##### 3.2. Effect of HCl concentration

The adsorption and separation performance of SIRs for In(III) and Fe(III) was studied in HCl solution. The existence form of In(III) and Fe(III) in HCl medium is very complicated. With increasing chloride concentration, In(III) or Fe(III) formed various  $\text{In}^{3+}-\text{Cl}^-$  or  $\text{Fe}^{3+}-\text{Cl}^-$  complexes in the aqueous phase. The effect of HCl concentration on adsorption was investigated. The effect of solution acidity on In(III) and Fe(III) in single-component system was studied by varying the hydrochloric acid concentration from 1 to 6 mol/L. The concentration of the metal ion solution used in this study was 60 mg/L

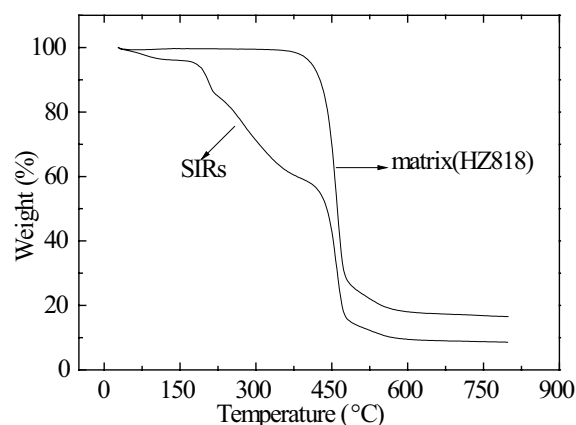


Fig. 4. Thermogravimetry analysis of SIRs and HZ-818 resin.

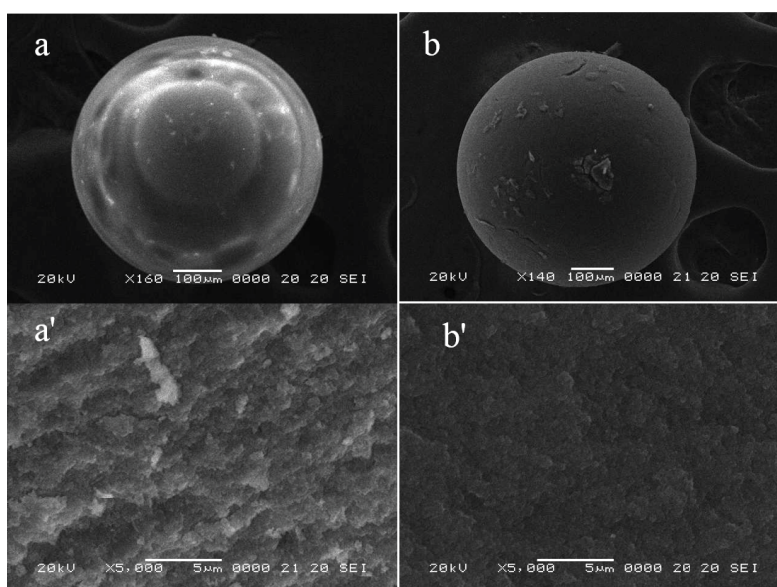


Fig. 3. Scanning electron microscope image of SIRs and HZ-818 resin (a, a': HZ-818 resin; b, b': SIR).

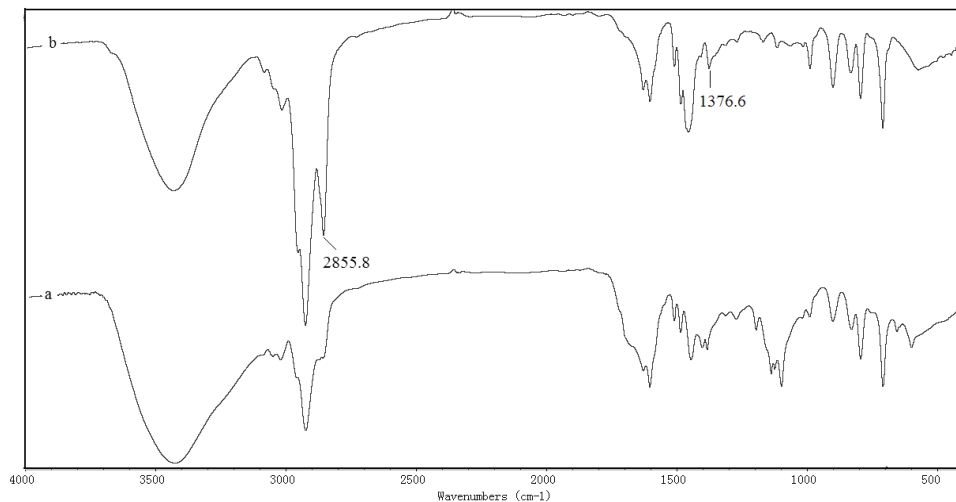


Fig. 5. Fourier transform infrared spectra of SIRs and HZ-818 resin (a: HZ-818 resin; b: SIRs).

at 298 K. Fig. 6 shows the effect of HCl concentration on the extraction of In(III) and Fe(III) in the single-component system. The adsorption capacity increased with increasing HCl concentration. The optimum adsorption solution acidity of SIRs for In(III) and Fe(III) is 4 mol/L HCl.

According to literature [20], In(III) exists in the form of  $\text{In}^{3+}$ ,  $\text{InCl}^{2+}$ ,  $\text{InCl}_2^+$ ,  $\text{InCl}_3$ , and  $\text{InCl}_4^-$  in HCl solutions. When the concentration of HCl is greater than 2 mol/L,  $\text{InCl}_4^-$  becomes the main species. Fe(III) in HCl solutions also exists in the form of  $\text{Fe}^{3+}$ ,  $\text{FeCl}^{2+}$ ,  $\text{FeCl}_2^+$ ,  $\text{FeCl}_3$ , and  $\text{FeCl}_4^-$  [33,34]. In 4 mol/L HCl medium,  $\text{InCl}_4^-$  and  $\text{FeCl}_4^-$  may be the probable chloro complex of indium and iron involved in adsorption [35,36].

The effects of solution acidity on In(III) and Fe(III) in the bi-component system were also studied. The adsorption capacities of In(III) and Fe(III) and separation coefficient  $\beta$  are shown in Fig. 7. SIRs exhibited better adsorption properties for Fe(III) than for In(III). Moreover, the separation coefficient  $\beta$  reaches the maximum value of 82 in 4 mol/L HCl. Hence, the optimal adsorption solution acidity was 4 mol/L HCl.

### 3.3. Dynamic adsorption

Static adsorption experiment can provide useful information on application to metal ion recovery, but dynamic adsorption experiments are closer to practical applications [37]. The breakthrough curve of metal ion adsorption on SIRs in dynamic adsorption process shows the effect of feed flow rate, bed height (mass of SIRs), and metal ions concentration.

#### 3.3.1. Single-component system

##### 3.3.1.1. Effect of feed flow rate

Feed flow rate is an important parameter of dynamic adsorption performance, which controls the adsorption time of metal ions on SIR. The effect of feed flow rate on the metal ion adsorption was studied by varying the feed

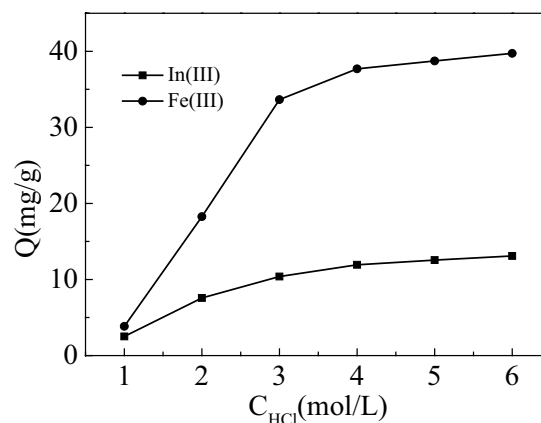


Fig. 6. Effect of HCl concentration on adsorption of In(III) and Fe(III) in single-component system.

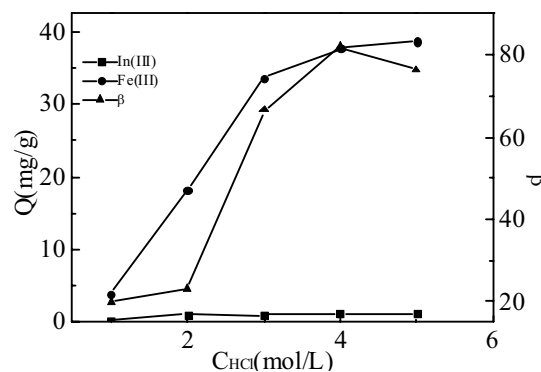


Fig. 7. Effect of HCl concentration on adsorption of In(III) and Fe(III) in bi-component system.

flow rate at 1.0–2.5 mL/min. Fig. 8 shows the breakthrough curves of different feed flow rates. Fig. 9 shows the effect of flow rates on the adsorption capacity of SIRs to In(III) and Fe(III). As shown in Fig. 8, the breakthrough curves

reached the breakthrough point more quickly when the feed flow rate was faster. As shown in Fig. 9, when the flow rate is 1.0 and 1.4 mL/min, the adsorption capacity does not change much. When the flow rate is greater than 1.4 mL/min, the adsorption capacity of SIRs to In(III) and Fe(III) decreased as the feed flow rate increased. This is caused by the decrease in contact time between metal ions and SIR as the feed flow rate increased. The feed flow rate of the subsequent dynamic adsorption experiment was 1.4 mL/min when comprehensively considering the adsorption amount and coefficient.

### 3.3.1.2. Effect of bed height

Another important parameter of dynamic adsorption performance is bed height. Fig. 10 shows the breakthrough curves of different bed heights, and Fig. 11 shows the adsorption capacity. As shown in Fig. 10a and b, the breakthrough point of In(III) and Fe(III) appeared at larger bed volume when the bed height was higher because the number of adsorption sites increased with increasing bed height. A high bed height can prolong the contact time between the metal ions and SIRs. However, the adsorption resistance also increased when the bed height was too high. As shown in Fig. 11, when the column height was 138 mm, the adsorption capacity of In(III) and Fe(III) was the largest. The optimum column height was 138 mm.

### 3.3.2. Bi-component system

The adsorption properties of In(III) and Fe(III) in bi-component system were studied by dynamic adsorption to determine the separation performance of SIRs for In(III) and Fe(III).

#### 3.3.2.1. Effect of feed flow rate

The breakthrough curves of In(III) and Fe(III) on SIRs at different feed flow rates are shown in Fig. 12. The concentration of In(III) in the effluent sample at feed flow rates of 1.0, 1.4, 2.0, and 2.5 mL/min was greater than the initial concentration from the effluent volumes of 90.4, 89.5, 91.0, and 78.8 mL, respectively. In(III) adsorbed on the SIRs were subsequently displaced by Fe(III). The SIRs could selectively absorb Fe(III) in bi-component system by dynamic

adsorption method. After adsorption, the SIRs were mainly loaded with Fe(III), and the adsorption capacities of Fe(III) were 36.4, 35.8, 30.8, and 28.7 mg/g at feed flow rates of 1.0, 1.4, 2.0, and 2.5 mL/min, respectively. However, the adsorption capacity of In(III) is very small (about 1–2 mg/g). Compared with that in the single-component system, the breakthrough curves also reached the breakthrough point more quickly when the feed flow rate was faster. The optimum feed flow rate was 1.4 mL/min under the experimental conditions.

#### 3.3.2.2. Effect of bed height

The breakthrough curves of different bed heights were studied. In Fig. 13a–c are the breakthrough curves of SIRs for In(III) and Fe(III) in the bi-component system at bed heights of 76 (300 mg), 140 (500 mg), and 190 (700 mg) mm, respectively. In Fig. 13, the breakthrough point appeared at a larger bed volume when the bed height was higher. In the bi-component system, In(III) adsorbed on the SIRs at bed heights of 76, 140, and 190 mm was subsequently displaced by Fe(III) with the ranges of 43.7–266, 89.8–359.2, and 132.7–480.2 mL. The SIRs could also selectively absorb Fe(III) at different bed heights. The break through point of In(III) and Fe(III) also appeared at a larger bed volume when the bed height

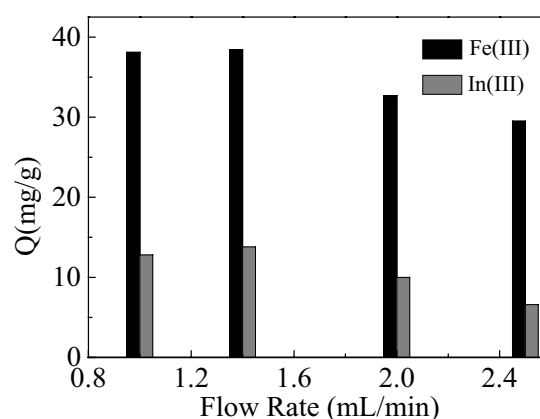


Fig. 9. Effect of flow rate on the adsorption capacity. ( $C_{\text{In(III)}}$ : 90 mg/L;  $C_{\text{Fe(III)}}$ : 90 mg/L;  $m$ : 500 mg).

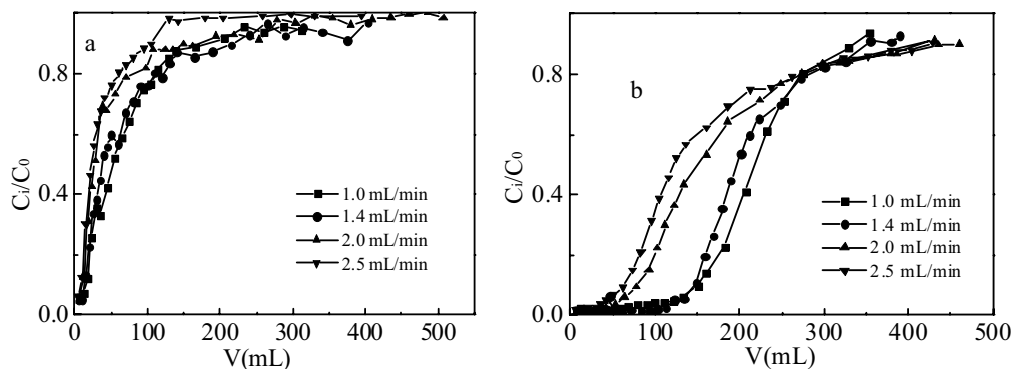


Fig. 8. Effect of the flow rate on the breakthrough curve (a: In(III); b: Fe(III)). ( $C_{\text{In(III)}}$ : 90 mg/L;  $C_{\text{Fe(III)}}$ : 90 mg/L;  $m$ : 500 mg).

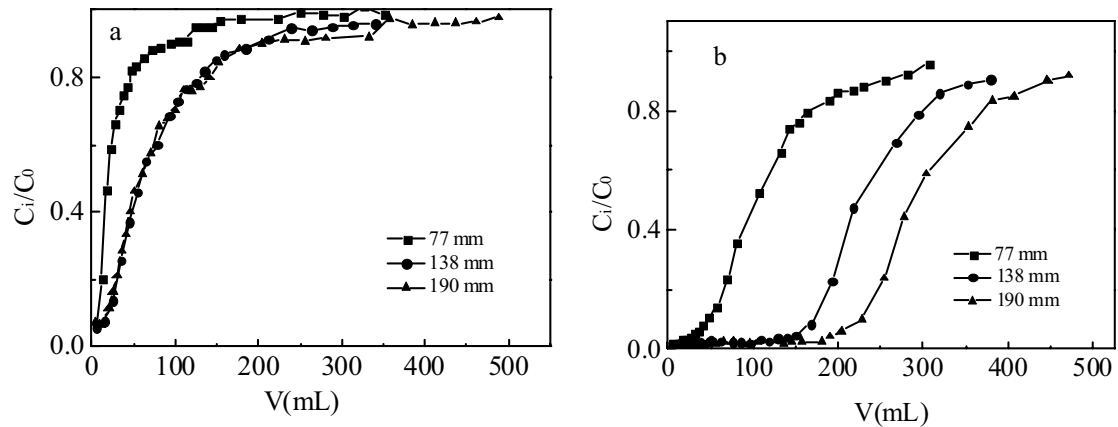


Fig. 10. Effect of bed height on the breakthrough curve (a: In(III); b: Fe(III)). ( $C_{In(III)}$ : 90 mg/L;  $C_{Fe(III)}$ : 90 mg/L; flow rate: 1.4 mL/min).

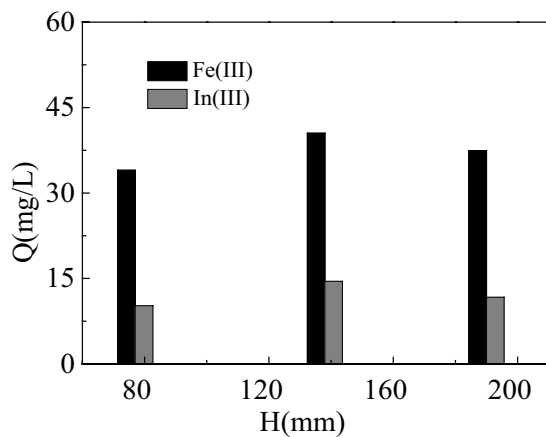


Fig. 11. Effect of bed height on the adsorption capacity. ( $C_{In(III)}$ : 90 mg/L;  $C_{Fe(III)}$ : 90 mg/L; flow rate: 1.4 mL/min).

was higher. Hence, the following adsorption experiments were carried out at a column height of 140 mm (500 mg).

### 3.3.2.3. Effect of metal ion concentration

The breakthrough curves of different metal ion concentration are shown in Fig. 14, where a, b, and c are the breakthrough curves of In(III) and Fe(III) adsorption onto SIRs at metal ion concentration of 60, 90, and 120 mg/L, respectively. The breakthrough point of In(III) and Fe(III) appeared at a larger bed volume when the concentration was lower because the driving force of SIRs for the adsorption of In(III) and Fe(III) increased with increasing metal ion concentration and the metal ions could occupy the adsorption sites faster. In addition, In(III) adsorbed on the SIRs at the metal ion concentrations of 60, 90, and 120 mg/L was subsequently displaced by Fe(III) from the volumes of 170.8, 92.0, and 88.3 mL, respectively. The SIRs could also selectively absorb Fe(III) at different metal ion concentrations. Hence, dynamic adsorption method was more applicable to adsorb metal ions of low concentration. However, the adsorption time increased when the

concentration was too low. In conclusion, the optimum metal ion concentration was 90 mg/L under the experimental conditions.

### 3.3.2.4. Dynamic adsorption under optimum conditions

The adsorption conditions were optimized. The optimum feed flow rate, bed height, and metal ion concentration are 1.4 mL/min, 140 mm, and 90 mg/L at ambient temperature, respectively. The adsorption properties of SIRs in single-component and bi-component systems were compared under the optimum adsorption conditions.

Fig. 15 shows the breakthrough curves of In(III) and Fe(III) in single-component and bi-component system under the optimum adsorption conditions. The adsorption capacities of In(III) and Fe(III) are 13.1 and 37.8 mg/g in the single-component system. However, the selective sorption of SIRs for Fe(III) in the bi-component system was found. Only In(III) was found in the effluent sample within the range of 0–86.5 mL in bi-component system, and In(III) adsorbed on the SIRs was subsequently displaced by Fe(III). The adsorption capacities of In(III) and Fe(III) were 1.3 and 35.8 mg/g in the bi-component system. The saturation capacity of SIRs for In(III) was lower in the co-existence of Fe(III). As such, separation of In(III) and Fe(III) was achieved.

### 3.4. Dynamic elution

SIRs loaded with In(III) or Fe(III) were eluted with HCl solution. The pH levels of the HCl solution were 1.0, 2.0, and 2.5, respectively. The results are shown in Fig. 16 and Table 1. In(III) or Fe(III) was eluted quite efficiently by HCl solution at pH 2.0 and 2.5. The elution rates for In(III) and Fe(III) were 99.7% and 100% at pH 2.5.

## 4. Conclusions

SIRs were prepared by dry impregnation with HZ-818 resin as support and trioctylmethylammonium chloride as extractant. The optimized acidity for In(III) and Fe(III) with SIRs was 4 mol/L HCl in single-component and bi-component systems. When HCl concentration was 4 mol/L, the optimized feed flow rate, bed height, and

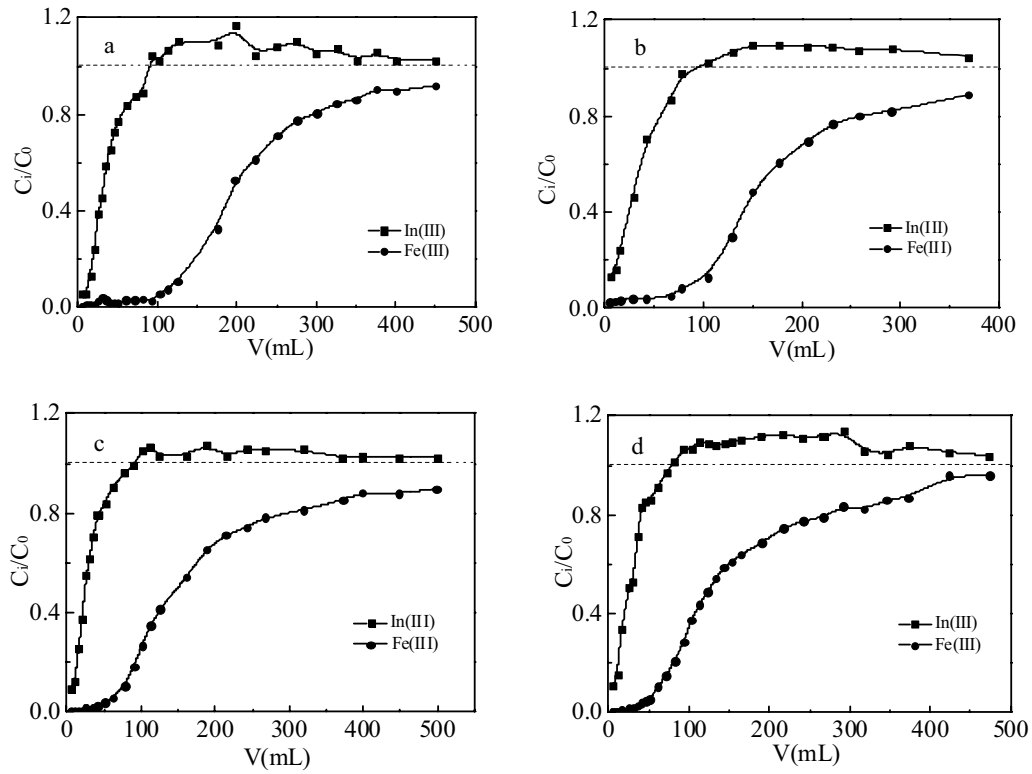


Fig. 12. Effect of feed flow rate on the breakthrough curve in bi-component system (a: 1.0 mL/min; b: 1.4 mL/min; c: 2.0 mL/min; d: 2.5 mL/min). ( $C_{In(III)}$ : 90 mg/L;  $C_{Fe(III)}$ : 90 mg/L;  $m$ : 500 mg).

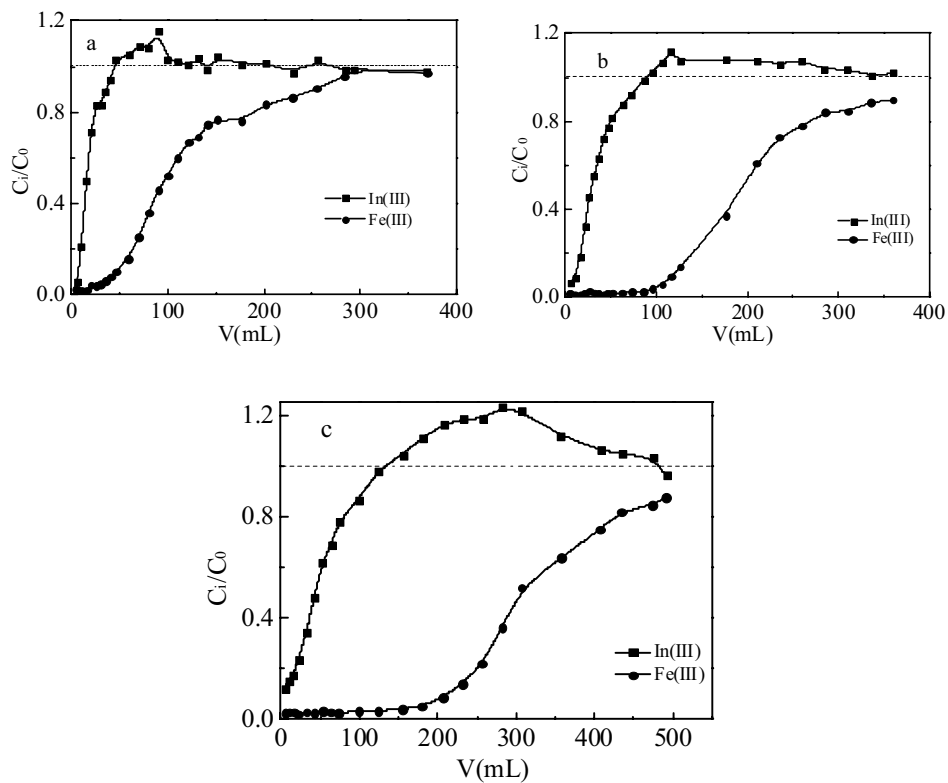


Fig. 13. Effect of bed height on the breakthrough curve in bi-component system (a: 76 mm; b: 140 mm; c: 190 mm). ( $C_{In(III)}$ : 90 mg/L;  $C_{Fe(III)}$ : 90 mg/L; flow rate: 1.4 mL/min).

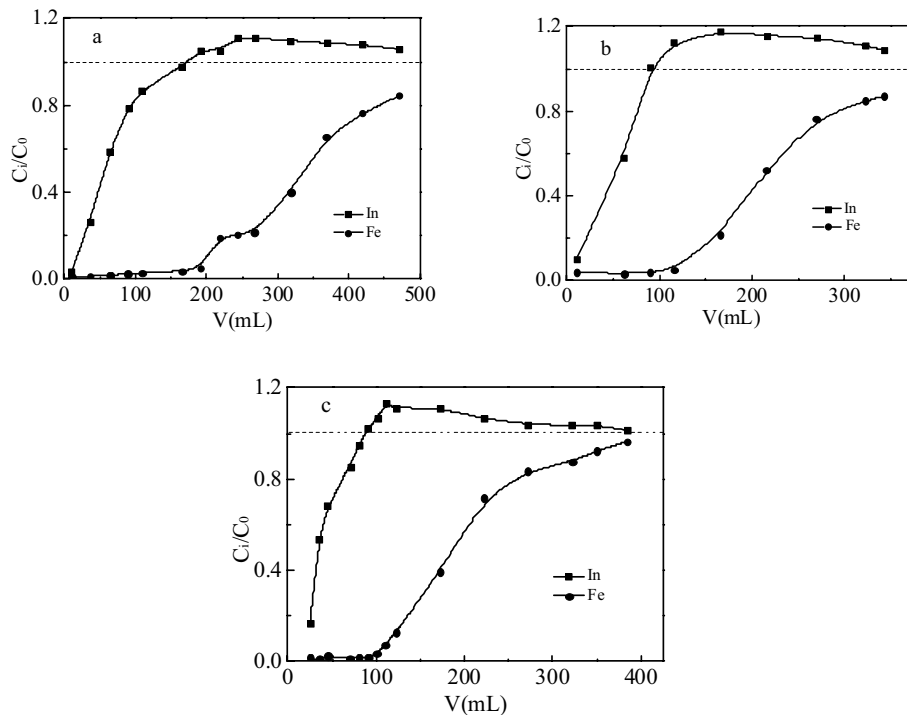


Fig. 14. Effect of the metal ion concentration on the breakthrough curve in bi-component system (a: 60 mg/L; b: 90 mg/L; c: 120 mg/L). (flow rate: 1.4 mL/min;  $m$ : 500 mg).

metal ion concentration were 1.4 mL/min, 140 mm, and 90 mg/L at ambient temperature, respectively. Under the optimized experimental conditions, the adsorption capacities of In(III) and Fe(III) in the single-component system were 13.1 and 37.8 mg/g, respectively. In the bi-component system, the SIRs had a high adsorption rate of Fe(III) at the initial stage of adsorption, and only In(III) was found in the effluent sample at the range of 0–86.5 mL. As the adsorption progressed, In(III) adsorbed on the SIR was subsequently displaced by Fe(III). SIRs could selectively adsorb Fe(III) in the bi-component system, and the adsorption capacities of In(III) and Fe(III) were 1.3 and 35.8 mg/g, respectively. Hence, SIRs can remove Fe(III) in the solution without losing In(III) in the solution. The separation of In(III) and Fe(III) occurred based on the selective adsorption of Fe(III) by SIR.

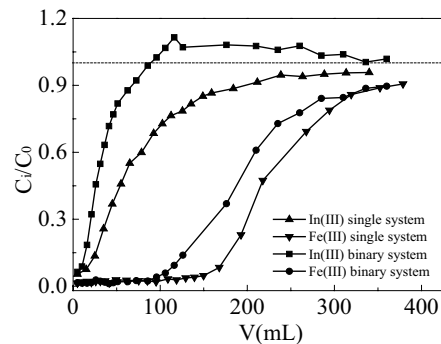


Fig. 15. Breakthrough curve in single-component and bi-component systems under the optimum adsorption conditions. ( $C_{In(III)}$ : 90 mg/L;  $C_{Fe(III)}$ : 90 mg/L; flow rate: 1.4 mL/min;  $m$ : 500 mg).

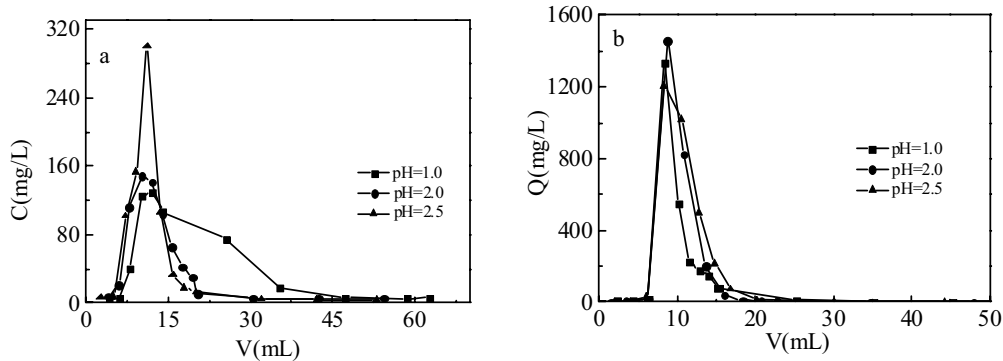


Fig. 16. Elution curves of SIRs after adsorption of In(III) and Fe(III) (a: In(III); b: Fe(III)).

Table 1  
Elution performance of different eluents

Elution rate	Eluent (HCl)	pH = 1.0	pH = 2.0	pH = 2.5
$E$ (%)	In(III)	82.6	97.7	99.7
	Fe(III)	71.3	90.8	100

### Acknowledgment

This project was supported by Natural Science Foundation of Shandong Province, China (No. ZR2018PB013), National Key Technology R&D Program (Grant No. 2015BAB02B03). The Yantai Key R&D Program, Shandong Province, China (No. 2017ZH062).

### Symbols

$Q$	– Adsorption capacity of metal ions on SIRs, mg/g
$C_0$	– Initial concentrations, mg/L
$C_e$	– Equilibrium concentrations, mg/L
$V$	– Volume of solution, L
$m$	– Mass of the SIRs, g
$D$	– Distribution ratio, L/g
$\beta$	– Separation coefficient
$C_i$	– Effluent sample concentrations of metal ions in dynamic adsorption process, mg/L
$V_i$	– Volume of effluent sample in dynamic adsorption process, L
$E$	– Dynamic elution rate, %
$C_j$	– Effluent sample concentrations of metal ions in dynamic elution process, mg/L
$V_j$	– Volume of effluent sample in dynamic elution process, L

### References

- [1] S.J.O. White, F.A. Hussain, H.F. Hemond, S.A. Sacco, J.P. Shine, R.L. Runkel, K. Walton-Day, B.A. Kimball, The precipitation of indium at elevated pH in a stream influenced by acid mine drainage, *Sci. Total Environ.*, 574 (2017) 1484–1491.
- [2] H. Hasegawa, I.M.M. Rahman, Y. Egawa, H. Sawai, Z.A. Begum, T. Maki, S. Mizutani, Chelant-induced reclamation of indium from the spent liquid crystal display panels with the aid of microwave irradiation, *J. Hazard. Mater.*, 254 (2013) 10–17.
- [3] N.T.T. Dang, D.-M. Wang, S.-Y. Huang, K.T. Tran, Indium recovery from aqueous solution containing oxalic acid – Enhancement by using hydrophobic membranes, *Sep. Purif. Technol.*, 235 (2020) 116300.
- [4] D. Pradhan, S. Panda, L.B. Sukla, Recent advances in indium metallurgy: a review, *Miner Process. Extr. Metall. Rev.*, 39 (2018) 167–180.
- [5] H. Murakami, S. Ishihara, Trace elements of Indium-bearing sphalerite from tin-polymetallic deposits in Bolivia, China and Japan: a femto-second LA-ICPMS study, *Ore Geol. Rev.*, 53 (2013) 223–243.
- [6] J. Yang, T. Retegan, B.-M. Steenari, C. Ekberg, Recovery of indium and yttrium from Flat Panel Display waste using solvent extraction, *Sep. Purif. Technol.*, 166 (2016) 117–124.
- [7] S. Dhiman, B. Gupta, Cyphos IL 104 assisted extraction of indium and recycling of indium, tin and zinc from discarded LCD screen, *Sep. Purif. Technol.*, 237 (2020) 116407.
- [8] X.B. Li, C. Wei, Z.G. Deng, C.X. Li, G. Fan, H. Rong, F. Zhang, Extraction and separation of indium and copper from zinc residue leach liquor by solvent extraction, *Sep. Purif. Technol.*, 156 (2015) 348–355.
- [9] T. Kinoshita, Y. Ishigaki, S. Kitagawa, R. Ichino, Y. Kamimoto, Selective recovery of indium via continuous counter-current foam separation from sulfuric acid solutions II – Optimization of operational parameters on separation performance, *Sep. Purif. Technol.*, 238 (2020) 116490.
- [10] M. Martin, E. Janneck, R. Kermer, A. Patzig, S. Reichel, Recovery of indium from sphalerite ore and flotation tailings by bioleaching and subsequent precipitation processes, *Miner. Eng.*, 75 (2015) 94–99.
- [11] C. Kim, C.R. Lee, J. Heo, S.M. Choi, D.H. Lim, J. Cho, S. Chung, J.R. Kim, Spontaneous and applied potential driven indium recovery on carbon electrode and crystallization using a bioelectrochemical system, *Bioresour. Technol.*, 258 (2018) 203–207.
- [12] X.B. Li, Z.G. Deng, C.X. Li, C. Wei, M.T. Li, G. Fan, H. Rong, Direct solvent extraction of indium from a zinc residue reductive leach solution by D2EHPA, *Hydrometallurgy*, 156 (2015) 1–5.
- [13] S.-K. Lee, U.-H. Lee, Adsorption and desorption property of iminodiacetate resin (Lewatit® TP207) for indium recovery, *J. Ind. Eng. Chem.*, 40 (2016) 23–25.
- [14] N. Kabay, J.L. Cortina, A. Trochimczuk, M. Streat, Solvent-impregnated resins (SIRs) – methods of preparation and their applications, *React. Funct. Polym.*, 70 (2010) 484–496.
- [15] S.X. Bao, Y.P. Tang, Y.M. Zhang, L. Liang, Recovery and separation of metal ions from aqueous solutions by solvent-impregnated resins, *Chem. Eng. Technol.*, 39 (2016) 1377–1392.
- [16] M. Paramanik, S. Panja, P.S. Dhama, J.S. Yadav, C.P. Kaushik, S.K. Ghosh, Unique reversibility in extraction mechanism of U compared to solvent extraction for sorption of U(VI) and Pu(IV) by a novel solvent impregnated resin containing trialkyl phosphine oxide functionalized ionic liquid, *J. Hazard. Mater.*, 354 (2018) 125–132.
- [17] S. İnan, H. Tel, Ş. Sert, B. Çetinkaya, S. Sengül, B. Özkan, Y. Altaş, Extraction and separation studies of rare earth elements using Cyanex 272 impregnated Amberlite XAD-7 resin, *Hydrometallurgy*, 181 (2018) 156–163.
- [18] Y.P. Tang, S.X. Bao, Y.M. Zhang, L. Liang, Effect of support properties on preparation process and adsorption performances of solvent impregnated resins, *React. Funct. Polym.*, 113 (2017) 50–57.
- [19] H.N. Kang, J.Y. Lee, J.Y. Kim, Recovery of indium from etching waste by solvent extraction and electrolytic refining, *Hydrometallurgy*, 110 (2011) 120–127.
- [20] J.X. Yang, T. Retegan, C. Ekberg, Indium recovery from discarded LCD panel glass by solvent extraction, *Hydrometallurgy*, 137 (2013) 68–77.
- [21] M.K. Sinha, S.K. Sahu, P. Meshram, B.D. Pandey, Solvent extraction and separation of zinc and iron from spent pickle liquor, *Hydrometallurgy*, 147–148 (2014) 103–111.
- [22] S.L. Wei, J.S. Liu, S.X. Zhang, X.L. Chen, Q.Q. Liu, L.L. Zhu, L. Guo, X.Y. Liu, Stoichiometry, isotherms and kinetics of adsorption of In(III) on Cyanex 923 impregnated HZ830 resin from hydrochloric acid solutions, *Hydrometallurgy*, 166 (2016) 205–213.
- [23] J.S. Liu, X.Z. Gao, C. Liu, L. Guo, S.X. Zhang, X.Y. Liu, H.M. Li, C.P. Liu, R.C. Jin, Adsorption properties and mechanism for Fe(III) with solvent impregnated resins containing HEHEHP, *Hydrometallurgy*, 137 (2013) 140–147.
- [24] Y.X. Yuan, J.S. Liu, B.X. Zhou, S.Y. Yao, H.M. Li, W.X. Xu, Synthesis of coated solvent impregnated resin for the adsorption of indium (III), *Hydrometallurgy*, 101 (2010) 148–155.
- [25] X. Zhang, K. Zhou, Y. Wu, Q. Lei, C. Peng, W. Chen, Separation and recovery of iron and scandium from acid leaching solution of red mud using D201 resin, *J. Rare Earth*, 38 (2020) 1322–1329.
- [26] L.J. Wang, Y. Wang, L. Cui, J.M. Gao, Y.X. Guo, F.Q. Cheng, A sustainable approach for advanced removal of iron from CFA sulfuric acid leach liquor by solvent extraction with P507, *Sep. Purif. Technol.*, 251 (2020) 117371.
- [27] G.P. Hu, Y. Wu, D.S. Chen, Y. Wang, T. Qi, L.N. Wang, Selective removal of iron(III) from highly salted chloride acidic solutions

- by solvent extraction using di(2-ethylhexyl) phosphate, *Front. Chem. Sci. Eng.*, (2020). <https://doi.org/10.1007/s11705-020-1955-4>.
- [28] M.Y. Li, Z.M. He, L. Zhou, Removal of iron from industrial grade aluminum sulfate by primary amine extraction system, *Hydrometallurgy*, 106 (2011) 170–174.
- [29] R.K. Mishra, P.C. Rout, K. Sarangi, K.C. Nathasarma, Solvent extraction of Fe(III) from the chloride leach liquor of low grade iron ore tailings using Aliquat 336, *Hydrometallurgy*, 108 (2011) 93–99.
- [30] L. Cui, Z.S. Zhao, Y.X. Guo, F.Q. Cheng, Stripping of iron(III) from iron(III)-loaded Aliquat 336 generated during aluminum recovery from coal waste leach liquor using sodium sulfite, *Sep. Purif. Technol.*, 199 (2018) 304–310.
- [31] K. Inoue, S. Alam, Hydrometallurgical recovery of indium from flat-panel displays of spent liquid crystal televisions, *Jom*, 67 (2015) 400–405.
- [32] S.V. Roosendaal, M. Regadío, J. Roosen, K. Binnemans, Selective recovery of indium from iron-rich solutions using an Aliquat 336 iodide supported ionic liquid phase (SILP), *Sep. Purif. Technol.*, 212 (2019) 843–853.
- [33] A. Agrawal, S. Kumari, K.K. Sahu, Studies on solvent extraction of iron(III) as a step for conversion of a waste effluent to a value added product, *J. Environ. Manage.*, 92 (2011) 3105–3111.
- [34] S.I. El Dessouky, Y.A. El-Nadi, I.M. Ahmed, E.A. Saad, J.A. Daoud, Solvent extraction separation of Zn(II), Fe(II), Fe(III) and Cd(II) using tributylphosphate and Cyanex 921 in kerosene from chloride, *Chem. Eng. Process.*, 47 (2008) 177–183.
- [35] C. Deferm, B. Onghena, T.V. Hoogerstraete, D. Banerjee, J. Luyten, H. Oosterhof, J. Fransaerc, K. Binnemans, Speciation of indium(III) chloro complexes in the solvent extraction process from chloride aqueous solutions to ionic liquids, *Dalton Trans.*, 46 (2017) 4412–4421.
- [36] X. Zhang, K. Zhou, Q. Le, Y. Huang, C. Peng, W. Chen, Selective removal of iron from acid leachate of red mud by Aliquat336, *Jom*, 71 (2019) 4608–4615.
- [37] J.N. Wang, L. Xu, Y. Meng, C. Cheng, A.M. Li, Adsorption of Cu<sup>2+</sup> on new hyper-crosslinked polystyrene adsorbent: Batch and column studies, *Chem. Eng. J.*, 178 (2011) 108–114.